Identification of Iron Species in Fe−BEA: Influence of the Exchange Level

M. Mauvezin,[†] G. Delahay,[†] B. Coq,*[,†] S. Kieger,[‡] J. C. Jumas,[§] and J. Olivier-Fourcade[§]

Laboratoire des Matériaux Catalytiques et Catalyse en Chimie Organique, UMR 5618 CNRS, ENSCM, 8 rue de l'Ecole Normale, 34296 Montpellier Cedex, France, Grande Paroisse S.A., Usine de Rouen, rue de l'Industrie, BP 204, 76121 Le Grand-Quevillly Cedex, France, and Laboratoire des Agrégats Moléculaires et Matériaux Inorganiques, UMR 5072, CNRS Université de Montpellier II, Place Eugène Bataillon, 34095 Monptellier Cedex 05, France

Received: June 16, 2000; In Final Form: November 21, 2000

A series of Fe−zeolite-beta (Fe−BEA and ^{57}Fe−BEA) has been prepared either by exchanging BEA (Si/Al = 12.5) with $Fe(NO_3)_3$ or by impregnation. The identification of Fe species in Fe−BEA has been carried out by temperature-programmed reduction (TPR) with H_2 or CO and Mössbauer and DRIFT spectroscopies after various pretreatments. These pretreatments consisted of the calcination by O_2, the reduction by H_2, and the calcination by N_2O of the prereduced sample. After calcination in O_2, Fe_2O_3 aggregates are only present when the exchange level exceeded 100%. At an exchange level lower than 100%, Fe would mainly be present as binuclear oxocations of the type $[(OH)FeOFe(OH)]^{2+}$, with the proportion decreasing as Fe content decreases. There are some unreducible Fe atoms, possibly in tetrahedral coordination in the zeolite framework. After the calcination in N_2O of prereduced Fe−BEA, the great difference stands in the formation of different Fe oxocations, much more easily reducible than those formed upon calcination in O_2. It is postulated that these specific oxocations would mainly be composed of mononuclear Fe species.

I. Introduction

Fe−zeolites have recently seen renewed interest due to their ability to catalyze selective reactions in various fields. Fe−ZSM-5 is particularly studied because of its promising behavior in hydrocarbon oxidation,[1] N_2O decomposition,[2] and the selective catalytic reduction of NO[3,4] and/or N_2O[5−7] by hydrocarbons or NH_3.[8,9] Particular attention has been paid to the specific formation of a reactive oxygen species, the so-called α-oxygen, by activation with N_2O.[1] It has been proposed that this α-oxygen would be associated with Fe in binuclear oxocations in Fe−ZSM-5[1,10−17] and Fe-ferrierite,[15,18] but it has never been identified in other Fe-zeolites. This shows the incidence of the zeolite structure on the stabilization of Fe cationic species and their reactivity. With regard to ZSM-5 and ferrierite, zeolite-beta (BEA) is attractive because of its widely open structure, comprising a three-directional channel system with 12-membered ring apertures,[19] with full accessibility to aluminum atoms and compensating cations in the structure. In addition, recent results indicate that some of the framework Al in zeolite BEA can move from tetrahedral to octahedral coordination upon exposure to oxygen ligands, thereby demonstrating the potential for unique Lewis acid properties[20] and better cation stabilization properties. A great number of exchanged cationic sites exist, and some of them exhibit a high adaptability.[21] These specific properties make Fe−BEA catalysts as attractive candidates for the above-mentioned reactions involving NO and/or N_2O. The effects of Fe loading and of pretreatments on the nature and reducibility of iron species in Fe−BEA have never been studied in detail until now. It was therefore the aim of this work by using complementary techniques: temperature-programmed reduction (TPR) by hydrogen or CO and ^{57}Fe Mössbauer and DRIFT spectroscopies.

* Corresponding author. Fax: +33 4 67 14 43 49. E-mail: coq@cit.enscm.fr.

[†] Laboratoire des Matériaux Catalytiques et Catalyse en Chimie Organique.

[‡] Grande Paroisse S.A, Usine de Rouen.

[§] Laboratoire des Agrégats Moléculaires et Matériaux Inorganiques, Université de Montpellier II.

II. Experimental Part

II.A. Materials. Depending on the metal loading chosen, different methods were carried out for the preparation of Fe(*x*)BEA, *x* being the theoretical degree of exchange ($x = 300$ Fe/Al, mol/mol). The chemicals used were H−BEA zeolite (PQ corporation zeolite CBV 810B-25, specific surface area = 680 $m^2\ g^{-1}$, Si/Al = 12.5) and $Fe(NO_3)_3 \cdot 9H_2O$ (Aldrich, 98+%).

For low exchange levels ($x < 100$), the samples were prepared by ion-exchange method and called Fe(*x*)BEAe. H−BEA (2 g) was added to 500 cm^3 of an $Fe(NO_3)_3$ aqueous solution ($0.5-2 \times 10^{-3}$ mol L^{-1}) and then stirred for 48 h; the pH of the slurry was kept at 3.8−4.0. After filtration, the solid was washed three times before being dried at 353 K in air. For Mössbauer experiments, the samples were prepared with 20 mg of ^{57}Fe for 1 g of zeolite, the excess being ^{56}Fe. A powder of ^{57}Fe was dissolved in hot concentrated HNO_3 and added to the slurry as usual. The materials are then called ^{57}Fe(*x*)BEAe.

Heavily loaded Fe(126)BEAi and Fe(375)BEAi were prepared by dry impregnation. H−BEA (2 g) was poured in 10 cm^3 of an $Fe(NO_3)_3$ aqueous solution; after evaporation the solid was dried at 353 K in air.

A 8.5%Fe_2O_3/BEA sample was obtained as a mechanical mixture of 17 mg of Fe_2O_3 (Prolabo) with 184 mg of H−BEA.

All the solids, with the exception of 8.5%Fe_2O_3/BEA, were calcined at 773 K in air (50 $cm^3\ min^{-1}$; ramp, 10 K min^{-1}).

II.B. Samples Characterization. The chemical analyses were performed at the Service Central d'Analyse du CNRS (Vernaison, France) by ICP (Table 1). All the materials were character-

10.1021/jp0021906 CCC: $20.00
Published on Web 01/17/2001

TABLE 1: Some Characteristics of Fe−BEA Samples at Different Fe Loadings

sample	chemical composition (wt %) Si	Al	Fe	theoretical exchange degree (%)	specific surface area[a] ($m^2\ g^{-1}$)
Fe(10)BEAe	35.00	2.64	0.19	10	618
Fe(24)BEAe	34.70	2.43	0.40	24	614
Fe(49)BEAe	35.45	2.65	0.90	49	609
Fe(79)BEAe	34.70	2.75	1.50	79	605
Fe(97)BEAe	39.75	2.86	1.91	97	600
Fe(126)BEAi	33.50	2.70	2.35	126	583
Fe(169)BEAi	33.00	2.75	3.20	169	587
Fe(375)BEAi	32.25	2.18	5.64	375	530
^{57}Fe(10)BEAe	32.00	2.60	0.18	10	−
^{57}Fe(24)BEAe	38.11	2.56	0.42	24	−
^{57}Fe(36)BEAe	37.84	3.38	0.85	36	−
^{57}Fe(119)BEAe	37.10	2.20	1.80	119	−
8.5%Fe_2O_3/BEA	34.35	2.80	5.50	−	−

[a] For the sake of simple comparison between the samples, the specific surface area was determined according to the BET method, even if this method has no physical meaning for N_2 adsorption in microporous zeolites.

ized by N_2 sorption at 77 K, DRX, TPR, and Mössbauer spectroscopy.

TPR by H_2 was carried out with a Micromeritics AutoChem 2910 apparatus using TCD detection. The H_2 consumption was determined after trapping H_2O at ca. 200 K. In each TPR experiment, there was a first peak appearing at ca. 300 K, which is due to the desorption of residual Ar, as proposed by Chen and Sachtler.[22] All the TPR profiles were computer-fitted and deconvoluted with the help of a least-squares fitting procedure assuming symmetrical profiles for the individual contributions.

In a first set of experiments, the TPR was carried out with H_2/Ar (25/75, vol/vol) in order to initiate below 1300 K the reduction to Fe^0 of the charge-compensating Fe^{3+} ion in Fe−BEA, whenever possible. In other experiments, the TPR was carried out with H_2/Ar (3/97, vol/vol) for better sensitivity and peak separation in the "low-temperature" region (< 800 K).

The TPR by H_2/Ar (25/75) was carried out after calcination of the 200 mg sample at 823 K in air for 2 h and then cooled to room temperature (RT) in air. After the sample is outflowed with air, the TPR is then started up to 1300 K (flow, 13 $cm^3\ min^{-1}$; ramp, 10 K min^{-1}).

The TPR by H_2/Ar (3/97) of the 200 mg sample was carried out after calcination in air at 823 K, and after activation in N_2O/He. In the case of activation in N_2O/He, the sample was first reduced for 2 h at 973 K in H_2/Ar (3/97). After cooling in H_2/Ar to RT, the sample was purged with He and then activated in N_2O/He (5/95) at 973 K for 2 h, and then it was cooled to 353 K in the same gas. After the sample was flushed with He, the TPR with H_2/Ar (3/97) was then started from 353 to 973 K (flow, 13 $cm^3\ min^{-1}$; ramp, 10 K min^{-1}).

To differentiate between naked Fe ions and oxocations after activation in air or N_2O, we carried out the TPR by CO/He (1/99) after exactly the same activation procedures as just above-described for the TPR by H_2/Ar (3/97). For these TPR experiments, the detection was processed by a Pfeiffer Omnistar QMS 200 mass spectrometer, and the masses 2 (H_2), 18 (H_2O), 28 (N_2 or CO), 30 (NO), 32 (O_2), and 44 (N_2O or CO_2) were followed. In all cases, H_2 release was observed at high temperature (T > 773 K), due to the water−gas shift reaction ($CO + H_2O \rightarrow CO_2 + H_2$). This contribution was tentatively eliminated by subtracting from the CO consumed an equal amount of the H_2 formed.

^{57}Fe Mössbauer experiments were performed at RT with an EG&G constant acceleration spectrometer in transmission mode. The source, of nominal activity 10 mCi, was ^{57}Co in a Rh matrix. The velocity scale was calibrated by using the standard magnetic sextuplet spectrum of a high-purity iron foil absorber. The origin of the isomer shift scale was determined from the center of the α-Fe spectrum, also recorded at RT. The absorbers were prepared from 1 g of catalyst in a specific Pyrex cell which can be sealed under controlled atmosphere. This cell was specially designed for these experiments. It is composed of two very thin 20 mm diameter Pyrex windows separated by 15 mm of Pyrex, with two connecting tubes allowing gas flow. All samples were pretreated at 823 K in air (flow, 50 $cm^3\ min^{-1}$; ramp, 10 K min^{-1}). The cell was then sealed and placed in the spectrometer for Mössbauer measurements. Experimental data were analyzed using the ISO software[23,24] by fitting the recorded spectra to Lorentzian profiles by the least-squares method. Goodness of fit was controlled by the classical x^2 test.

In situ DRIFT experiments were conducted on a Bruker Equinox 55 spectrometer with a special cell (Graseby Specac) with flowing gas and operating at high temperature. Fe−BEA/CaF_2 (40/60, 50 mg) was placed in the cell, and the spectra (100 scans) were collected after treatments at 673 K in (i) Ar, (ii) air, (iii) N_2O/He after reduction in H_2/Ar, and (iv) H_2/Ar, according to the procedures described above for TPR experiments by H_2/Ar (3/97).

III. Results and Discussions

Our purpose was to identify the nature of Fe species in Fe−BEA, depending on Fe loading and nature of the oxidizing treatment (O_2 or N_2O). The discussion will be separated in two parts. The first part will deal with the nature of Fe species in Fe−BEA after calcination in air, and the second will deal with that after N_2O treatment.

III.A. Nature of Fe Species after Calcination in Air. The X-ray diffraction patterns of Fe−BEA only revealed the diffraction peaks of the host BEA structure. We never observed any diffraction line corresponding to iron oxide crystallites, even in the catalysts prepared by impregnation which contain more iron than the total exchange capacity allows. This implies that Fe_2O_3 aggregates are composed of very small crystallites (< 3 nm), or disordered aggregates. The absence of large Fe_2O_3 aggregates is in agreement with the near constancy of the surface area of Fe−BEA when Fe content is increased (Table 1). Figure 1 shows the TPR profiles of Fe−BEA by H_2/Ar (25/75), and Figures 2 and 3 show the Mössbauer spectra of ^{57}Fe−BEA. The H_2/Fe values for each H_2-consumption peak in TPR profiles are reported in Table 2.

III.A.1. 8.5%Fe_2O_3/BEA. The H_2-TPR profile of 8.5%Fe_2O_3/BEA, a reference material, is shown in Figure 1. Two peaks are observed; the first, at ca. 620 K, stands for the reduction of Fe_2O_3 in Fe_3O_4 ($3Fe_2O_3 + H_2 \rightarrow 2Fe_3O_4 + H_2O$, $H_2/Fe = 0.17$), which is in turn reduced to Fe^0 in one step ($Fe_3O_4 + 4H_2 \rightarrow 3Fe^0 + 4H_2O$, $H_2/Fe = 1.33$). This latter broad peak with maximum at ca. 780 K can be deconvoluted in two contributions, one centered at 700 K ($H_2/Fe = 0.27$), corresponding to the reduction of Fe_3O_4 in FeO, and another at 780 K ($H_2/Fe = 1.06$), corresponding to the reduction of FeO in Fe^0. These results are in agreement with previous works on the TPR by H_2 of various supported or unsupported iron oxides.[25−31]

III.A.2. Exchanged Fe(x)BEAe and ^{57}Fe(x)BEAe. Mössbauer spectra of ^{57}Fe(*x*)BEAe (Figure 2) only exhibit a broad doublet with isomer shifts (δ) of ca. 0.34 mm s^{-1} and quadrupole splittings (Δ) of ca. 1.1 mm s^{-1}. Such values are characteristics of Fe^{III} in distorted octahedral environments.[13,32−36] The absence of a sextuplet in the spectra of all samples for experiments

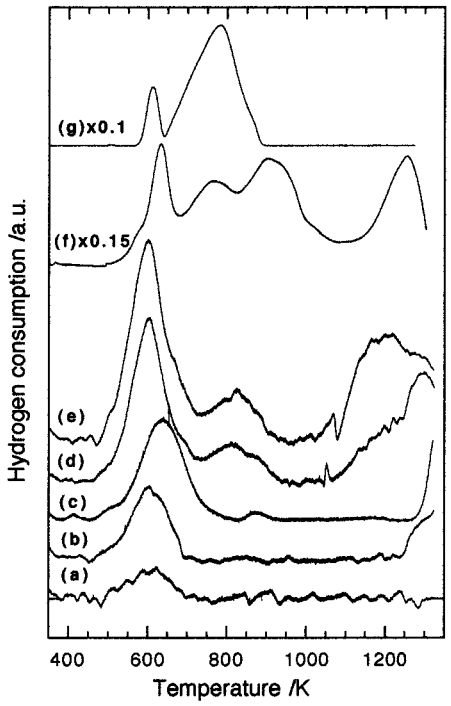

Figure 1. H_2-TPR profiles of calcined Fe−BEA catalysts: (a) Fe(24)BEAe, (b) Fe(49)BEAe, (c) Fe(97)BEAe, (d) Fe(126)BEAi, (e) Fe(169)BEAi, (f) Fe(375)BEAi, and (g) 8.5%Fe_2O_3/BEA. Conditions, H_2/Ar (25/75); ramp, 10 K min^{-1}.

TABLE 2: H_2/Fe and CO/Fe Molar Ratio Values during the TPR by H_2/Ar (3/97) and CO/He (1/99) of Calcined Fe(*x*)BEA Samples

		H_2−TPR			
		H_2/Fe			
sample	exchange level (%)	at $T <$ 973 K[a]	H_2/$Fe_{(total)}$[b]	Fe_2O_3/"Fe^{3+}"[c]	CO-TPR CO/Fe
Fe(10)BEAe	10	−	−	−	0.25
Fe(24)BEAe	24	0.25	0.25	0/100	0.15
Fe(49)BEAe	49	0.32	0.69	0/100	0.34
Fe(97)BEAe	97	0.42	1.08	1/99	0.42
Fe(126)BEAi	126	0.46	0.88	18/82	0.41
Fe(169)BEAi	169	0.44	0.79	41/59	−
Fe(375)BEAi	375	0.88	1.37	70/30	0.16
8.5%Fe_2O_3/BEA	−	−	1.50	100/0	0.14

[a] From TPR by H_2/Ar (3/97). [b] From TPR by H_2/Ar (25/75). [c] Proportion of Fe as Fe_2O_3 and "Fe^{3+}" species, "Fe^{3+}" including the unreducible species and oxocations (from TPR by H_2/Ar (25/75)).

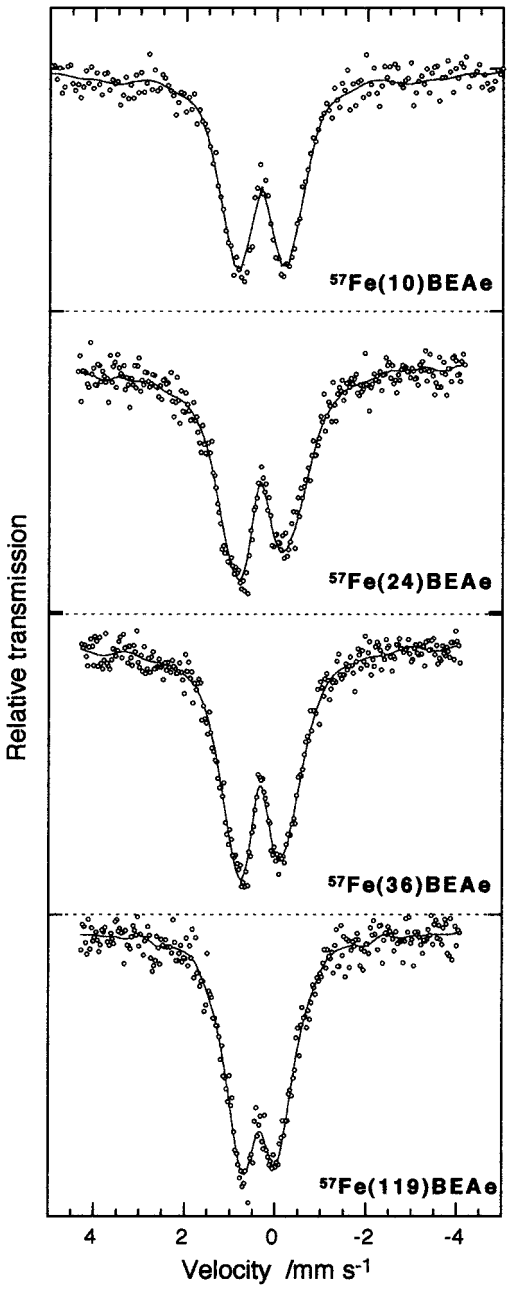

Figure 2. Mössbauer spectra of some calcined and dehydrated Fe−BEA catalysts.

carried out at room temperature and in ^{57}Fe(36)BEAe for an experiment carried out at 77 K rules out the presence of Fe_2O_3 aggregates with sizes larger than 10 nm.[37] Moreover, if Fe_2O_3 aggregates exist with sizes in the range of 3−10 nm, they should exhibit disordered structure due to the absence of any diffraction line in XRD experiments. As previously said, the broadening of doublet peaks provides evidence of Fe in distorted octahedral environment or the occurrence of several different Fe^{III} species. Figure 3 indeed shows the Mössbauer spectrum of ^{57}Fe(36)-BEAe with a deconvolution into three Lorentzian contributions with values of δ of 0.34, 0.34, and 0.27 mm s^{-1} and Δ values of 0.72, 1.43, and 2.26 mm s^{-1}. All the spectra from Figure 2 can be thus deconvoluted into three contributions, the δ and Δ values of which are given in Table 3, as well as the respective proportions of the corresponding Fe^{III} species. A δ value below 0.3 mm s^{-1} is indicative of Fe in a tetrahedral environment, likely incorporated in lattice position in zeolites.[38] It is worth noting that the proportion of these species does not change much from sample to sample. The widening of quadrupole splitting is indicative of Fe^{III} species with increasing distortion in both octahedral and tetrahedral environments. The doublet with δ = 0.25−0.32 mm s^{-1} and Δ = 1.9−2.2 mm s^{-1} might thus be attributed to Fe in highly distorted framework positions, which, however, never exceeded 16% in proportion (Table 3). Otherwise, these different contributions may also correspond to Fe^{3+} species in different cation charge compensation positions. It has indeed been proposed that nine unequivalent crystallographic tetrahedral (TO_4) sites exist in zeolite BEA,[39] which can be classified into three groups of similar structural parameters.[21]

To get more insight about the nature of Fe in Fe(*x*)BEAe, we carried out DRIFT experiments on some calcined samples (Figure 4). After dehydration in flowing dry Ar at 773 K for 2 h, the samples exhibit the expected bands in the OH stretching vibration region. The band at 3730 cm^{-1} is assigned to terminal Si−OH groups present in the channels and at the external surface, and that at 3600 cm^{-1} is assigned to isolated bridging

TABLE 3: Values of Isomer Shift (δ), Quadrupole Splitting (Δ), and Proportion of Fe Species Responsible for the Contribution of Each Deconvolution Doublet for Mössbauer Measurements of ^{57}Fe−BEA Catalysts

	first doublet			second doublet			third doublet				
sample	δ (mm/s)	Δ (mm/s)	(%)[a]	δ (mm/s)	Δ (mm/s)	(%)[a]	δ (mm/s)	Δ (mm/s)	(%)[a]	LW[b](mm/s)	x^2
^{57}Fe(10)BEAe	0.34(1)	0.78(2)	52.7	0.34(2)	1.44(4)	38.1	0.32(5)	2.24(9)	9.2	0.51(2)	0.51
^{57}Fe(24)BEAe	0.36(2)	0.73(3)	47.1	0.33(2)	1.43(4)	36.3	0.25(3)	2.11(6)	16.7	0.54(4)	0.86
^{57}Fe(36)BEAe	0.34(1)	0.72(2)	55.9	0.34(2)	1.43(3)	35.5	0.27(4)	2.26(7)	8.6	0.53(3)	0.70
^{57}Fe(119)BEAe	0.36(2)	0.55(3)	54.6	0.32(2)	1.12(5)	33.3	0.27(4)	1.94(7)	12.1	0.55(4)	0.49
Fe(375)BEAi	central doublet:			0.34(1)	0.75(1)	53.3	LW = 0.63 (2), x^2 = 0.84				
	sextuplet (HF = 49.7 T)[c]			0.38(2)	−0.09(1)	46.7	LW = 0.63(2)				

[a] Proportion in mol % of Fe present in these species. [b] LW: line width constained to be equal for all components. [c] HF: hyperfine field.

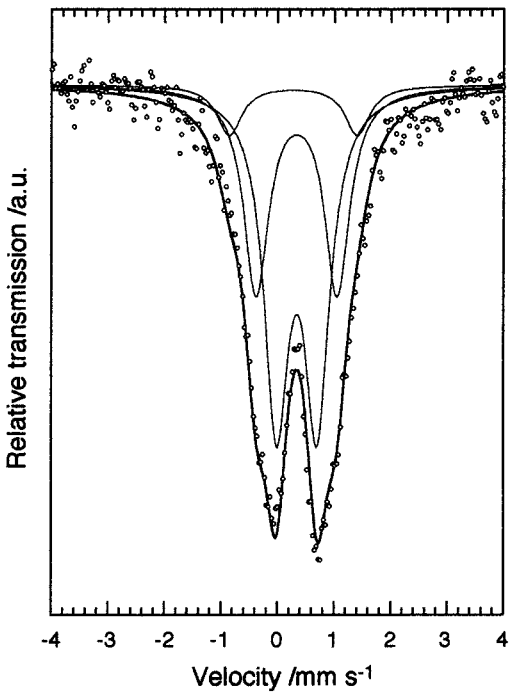

Figure 3. Mössbauer spectrum of calcined and dehydrated ^{57}Fe(36)-BEAe deconvoluted in three Lorentzian contributions doublets.

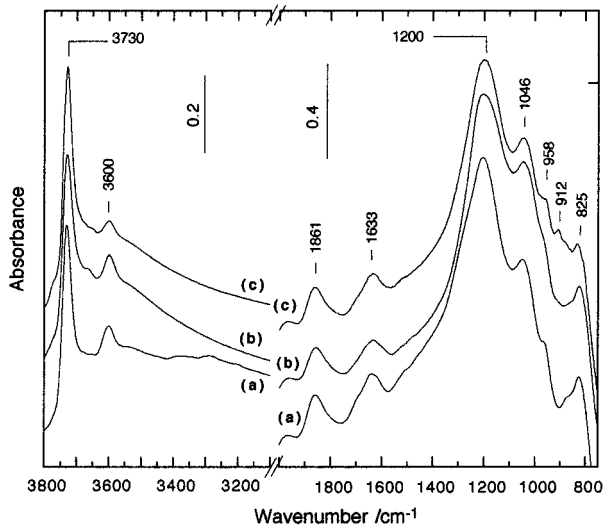

Figure 4. DRIFT spectra of (a) H−BEA, (b) Fe(10)BEAe and (c) Fe(97)BEAe calcined and dehydrated at 673 K.

acidic hydroxyl stretching vibrations (Si(OH)Al). A broad massif between 3300 and 3700 cm^{-1} is likely due to framework Si−OH, as well as to Si(OH)Al groups in interaction at defect sites.[20,40] It was shown that due to the presence of these defect sites in high proportion, there is not any clear correlation between the intensity of the band at 3600 cm^{-1} and the exchange capacity of H−BEA.[40] However, the relative decrease of this band intensity, compared to that at 3730 cm^{-1}, upon Fe loading provides evidence of the exchange by Fe species of at least a great proportion of isolated bridging protons (Si(OH)Al). In the framework vibrational frequency range, we can notice the appearance of a band at 912 cm^{-1} upon Fe loading. It can be assigned to the T−O−T framework vibration perturbed by Fe cationic species, as already suggested for Cu−ZSM-5,[41] Ga−ZSM-5,[42] and Co−BEA.[43]

In the H_2-TPR of Fe(97)BEAe, three peaks of hydrogen consumption are detected at ca. 630, 820, and 1330 K. In agreement with previous works on the H_2-TPR of Fe−ZSM-5[22,42−46] and of Fe−Y,[47] the first peak of hydrogen consumption would correspond to reduction of Fe^{3+} in Fe^{2+} and the high-temperature reduction peak to reduction of Fe^{2+} in Fe^0 upon the collapse of the zeolite network. The small H_2 consumption between 750 and 920 K points out the presence of some Fe_2O_3 aggregates in Fe(97)BEAe, in agreement with the redox behavior of 8.5%Fe_2O_3/BEA in H_2-TPR (section III.A.1). The corresponding H_2 consumption for the reduction of Fe_2O_3 to FeO is actually in the broad peak centered at 630 K and mainly due to the reduction of cationic Fe species. The proportion of Fe as Fe_2O_3 in the sample can thus be estimated; it is given in Table 2 as well as the total H_2 consumption in H_2-TPR. The data from Table 2 and Figure 1 show that (i) trace amounts of Fe_2O_3 are only present in Fe(97)BEAe, (ii) the reduction of Fe^{2+} to Fe^0 did not occur for Fe(24)BEAe, and (iii) the H_2 taken up in the LT peak (600−630 K), expressed as H_2/Fe, remains lower than 0.5; this can be due to the presence of either still reduced or unreducible Fe species. This latter proposition would be in better conformity with Mössbauer spectroscopy, since only Fe^{III} species were detected. The TPR data presented in Table 2 provide evidence that cationic species alone are present until a degree of exchange of 97% (300Fe/Al), which prompts us to think intuitively that naked Fe^{3+} cations would be exchanged during the preparation step. Actually, the chemistry of iron species in solution is extremely complex,[38,48] and $Fe(OH)^{2+}$, $Fe(OH)_2^+$, or $[Fe_2(OH)_2]^{4+}$ could exist in the pH range 3.5−4, depending on the Fe concentration. At the low Fe concentrations used, the first species should prevail in comparison to the latter, which, moreover, could be more difficult to exchange due to its high positive charge. Anyway, the iron can be introduced either as $Fe(OH)^{2+}$ or as $[Fe_2(OH)_2]^{4+}$; this actually corresponds to a maximum degree of exchange of 65% protons for the final sample Fe(97)BEAe. A better description of cationic Fe species reduced at ca. 600−630 K, naked Fe^{3+} ions or oxocations, could be reached from CO-TPR experiments, since only an oxygen-containing Fe species can be reduced by CO.[47] With this end in view, we carried out TPR by H_2/Ar (3/97) and CO/He (1/99) up to 973 K. The CO-TPR profiles are exemplified for Fe(97)BEAe in Figure 5, and the normalized values for H_2 and

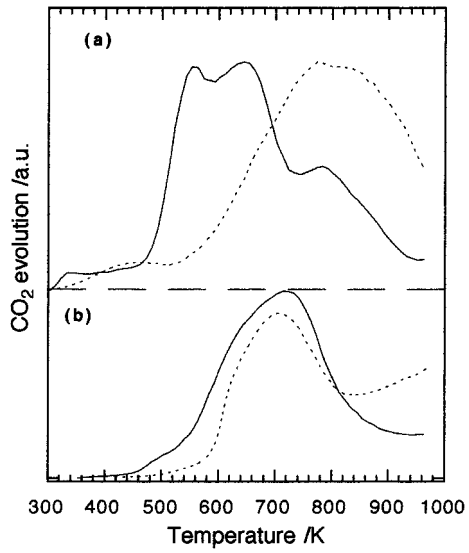

Figure 5. CO-TPR profiles of (a) Fe(97)BEAe and (b) Fe(375)BEAi (dotted lines) after calcination in air and (full lines) after oxidation by N_2O of the prereduced sample. Conditions, CO/He (1/99); ramp, 10 K min^{-1}.

CO uptakes given in Table 2. As mentioned above, it is worth noting that some CO_2 is formed at high temperature (> 800 K) from the reaction of CO with H_2O (water−gas shift reaction), with the concurrent release of H_2. The contribution of this reaction to CO_2 formation was then taken into account, but it introduced some uncertainties in the CO/Fe values. It comes out that the values of H_2/Fe (at T < 973 K) and CO/Fe for the reduction of exchanged Fe(x)BEAe (x < 100) can be seen as comparable. This behavior indicates that nearly all the reducible Fe species are composed of oxocations. For Fe(x)BEAe, the H_2/Fe and CO/Fe values tend to level off at 0.45−0.5 at a high degree of exchange, providing evidence of the likely occurrence of species containing one O for two Fe. We can assume that these species are probably binuclear oxocations with FeOFe bridges, as proposed by Garten et al.[50] in Fe−FAU. From a statistical point of view, one can expect that the proportion of binuclear complexes should decrease with decreasing Fe content if Fe ions are located at random at the cation sites; the H_2/Fe and CO/Fe values indeed decrease with the Fe content. From both experimental and theoretical studies, several structures of binuclear Fe oxocations with FeOFe bridges have been proposed as occurring in Fe−zeolite.[1,4,14,22,44,51] With regards to charge compensation, the dipositive complex $[(OH)FeOFe(OH)]^{2+}$ which requires only two Al centered tetrahedra in its proximity appears as a good candidate. It was proposed as the active site in Fe−ZSM-5 for the selective catalytic reduction of NO by hydrocarbons.[44] This proposition is not in contradiction with the above-suggested possibility that Fe would be introduced as $Fe(OH)^{2+}$ or $Fe(OH)_2^{+}$ rather than $[Fe_2(OH)_2]^{4+}$; the species $[(OH)FeOFe(OH)]^{2+}$ could indeed be formed between neighborood Fe species during the activation process.

III.A.3. Impregnated Fe(x)BEAi. Figure 6 shows the Mössbauer spectrum of Fe(375)BEAi and Figure 1 the H_2-TPR profiles of Fe(x)BEAi (x = 126, 169 and 375), with the corresponding H_2 consumptions in Table 2. The Mössbauer spectrum exhibits a sextuplet and a central doublet, with the δ and Δ values given in Table 3. In agreement with literature, the sextuplet is assigned to octahedral Fe^{III} in Fe_2O_3 aggregates with sizes larger than 13 nm.[37] Moreover, from the absence of the Fe_2O_3 diffraction line in the DRX pattern of Fe(375)BEAi, these aggregates exhibit an amorphous structure. Otherwise, the

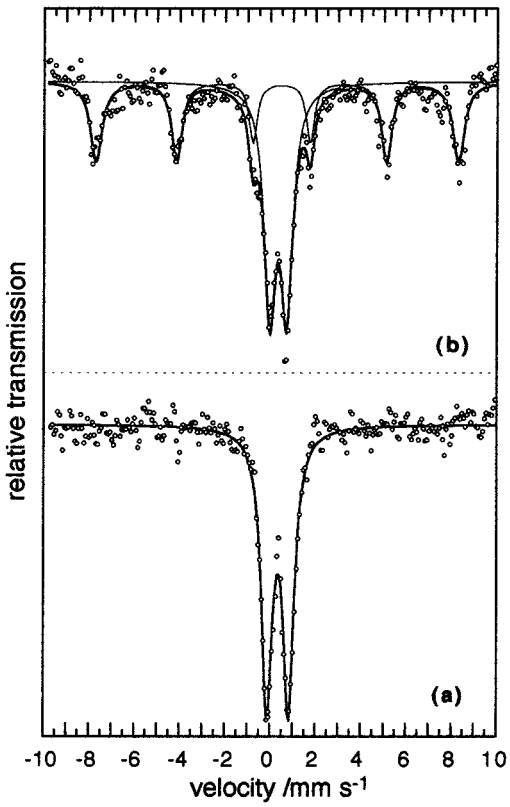

Figure 6. Mössbauer spectra of calcined and dehydrated (a) Fe(97)-BEAe and (b) Fe(375)BEAi.

central doublet, with isomer shift and quadrupole splitting very similar to those found for Fe in ^{57}Fe(x)BEAe, can be convincingly assigned to Fe^{III} in oxocations of various compositions as described above.

The H_2-TPR profiles of impregnated samples (Figure 1) show three or four H_2 consumption peaks. In the typical example of Fe(126)BEAi, three peaks are obtained:
(1) at ca. 600 K (with H_2/Fe = 0.40) for the reduction of Fe^{3+} in Fe^{2+} and of Fe_2O_3 in Fe_3O_4. We can observe a small shoulder centered around 690 K corresponding to the reduction of Fe_3O_4 in FeO.
(2) at ca. 800 K (H_2/Fe = 0.18) for the reduction of FeO in Fe^0.
(3) at 1200−1300 K (H_2/Fe = 0.30) for the reduction of Fe^{2+} in Fe^0 with the concurrent collapse of the zeolite network.

The total H_2 consumption provides evidence of the occurrence of unreducible Fe species in the impregnated samples too. The amount of H_2 taken up during the reduction peak lying from 800 to 900 K ($FeO \rightarrow Fe^0$) allows for estimating the amount of Fe_2O_3 aggregates. The proportion of cationic Fe species and Fe_2O_3 aggregates is thus given in Table 2, and a good fit exists between a near full exchange of H−BEA with Fe^{III} and the proportion of Fe as cations. This provides evidence of the high affinity of iron for exchanging protons in BEA zeolite.

In summary, depending on the preparation method and the wt % Fe, iron in calcined Fe−BEA materials is present as various species: (i) possibly some unreducible framework tetrahedral Fe species, (ii) Fe^{III} in binuclear oxocations, and (iii) Fe^{III} in amorphous Fe_2O_3 aggregates. Moreover, we have shown that the proportion of Fe^{III} in binuclear oxocations increases with the Fe content.

III.B. Nature of Fe Species after Treatment with N_2O. Mössbauer spectroscopy has been carried out on ^{57}Fe(24)BEAe, first reduced in H_2/Ar and then activated in N_2O/He. The

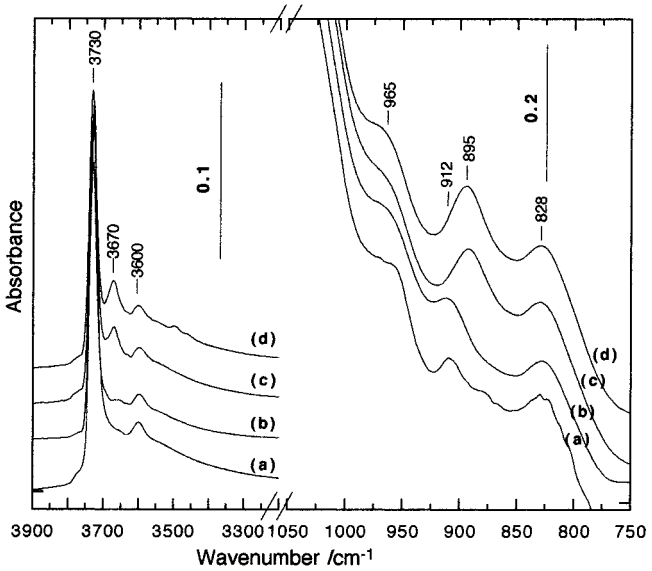

Figure 7. DRIFT spectra of Fe(97)BEAe after different treatments: (a) dehydration in Ar, (b) reduction in H_2, (c) calcination in air, and (d) oxidation in N_2O of the prereduced sample.

spectrum looks like that of the sample calcined in air, exhibiting a broad doublet with an isomer shift of 0.35 mm s^{-1} and a quadrupole splitting of 1.8 mm s^{-1}. This doublet can also be deconvoluted in three different contributions with δ values of 0.38, 0.29, and 0.31 mm s^{-1} and Δ values of 1.09 and 1.70, and 2.70 mm s^{-1}. The isomer shift values are close to those found on the calcined sample and characteristics of Fe^{III}, but the quadrupole splittings are wider, providing evidence of a more distorted environment. After treating Fe^{2+}−ZSM-5 with N_2O, Ovanesyan et al.[13] reported a Mössbauer spectrum with different doublet contributions. Interpretation of the resulting spectrum indicates either the appearance of two states of Fe^{3+} or the nonequivalence of the two Fe^{3+} ions involved in a same complex. The global δ and Δ values reported were 0.55 and 1.04 mm s^{-1}, which differ from those we have found.

There are some significant changes in the DRIFT spectra of Fe(*x*)BEAe depending on the activation treatment. This is shown in Figure 7 for Fe(97)BEAe after (i) dehydration in Ar, (ii) calcination in O_2, (iii) reduction in H_2, and (iv) treatment in N_2O after a prereduction step. Several specific features are relevant:

(1) A band at 3670 cm^{-1} appears after treatment in O_2 and N_2O but does not exist after H_2 treatment. This band likely corresponds to OH groups bonded either on extraframework Al species[20] or on Fe^{III} species. From quantum chemical calculations (DFT method) on small iron-hydroxo clusters, it was found that ν_{OH} in Fe−OH groups would exhibit a frequency at ca. 3670 cm^{-1}.[52] Otherwise, in Ga−ZSM-5, a band at 3660 cm^{-1}, appearing after reduction of the material, was assigned to Ga−OH groups.[41,53]

(2) A band at 895 cm^{-1} appears after treatment in air or N_2O, which vanishes at the benefit of a band at ca. 912 cm^{-1} after reduction. As mentioned above, this band can be assigned to T−O−T framework vibrations perturbed by Fe species. One could postulate that the change of ν_{TOT} from 895 to 912 cm^{-1} comes from either the oxidation state of Fe or its coordination.

Finally, the adsorption of CO after the various treatments of Fe(97)BEAe has been followed by DRIFT to identify the occurrence of Lewis sites and of the Fe carbonyl species. CO adsorbed on Fe(97)BEAe is only detected after treatment by N_2O with a band at 2233 cm^{-1}, typical of CO on Lewis sites.

The H_2-TPR and CO-TPR have been carried out on the N_2O-treated Fe−BEA. Typical TPR profiles are shown in Figures 5 and 8 for CO and H_2, respectively, and the H_2 and CO taken up during these experiments are given in Table 4. The H_2-TPR was carried out with H_2/Ar (3/97), with the aim to reach a higher sensitivity and better resolution in the low-temperature range. Under these conditions, the reduction step $Fe^{2+} \rightarrow Fe^0$ was never achieved, but a subsequent H_2-TPR with H_2/Ar (25/75) did not

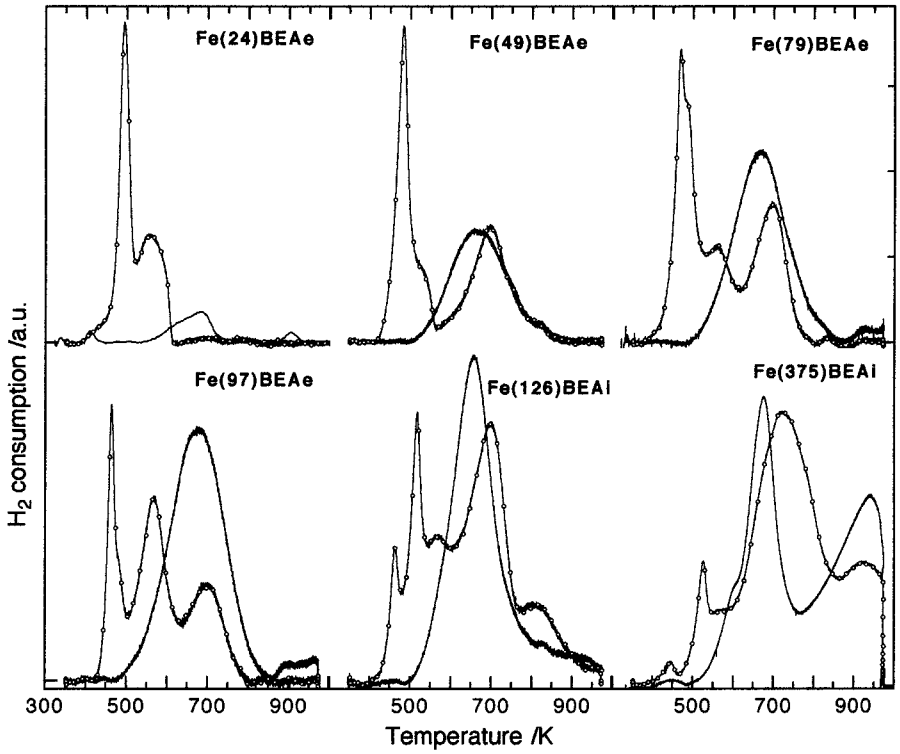

Figure 8. H_2-TPR profiles of Fe−BEA catalysts after different treatments: (—) calcination in air and (—o—) oxidation in N_2O of the prereduced sample. Conditions, H_2/Ar (3/97); ramp, 10 K min^{-1}.

TABLE 4: H_2/Fe and CO/Fe Molar Ratio Values during the TPR by H_2/Ar (3/97) and CO/He (1/99) of Fe(*x*)BEA Samples Treated by N_2O after Reduction by H_2

sample	H_2/Fe (H_2−TPR)	CO/Fe (CO-TPR)
Fe(10)BEAe	−	0.75
Fe(24)BEAe	1.00	0.45
Fe(49)BEAe	0.60	0.50
Fe(79)BEAe	0.70	−
Fe(97)BEAe	0.26	0.33
Fe(126)BEAi	0.49	0.64
Fe(375)BEAi	0.53	0.31

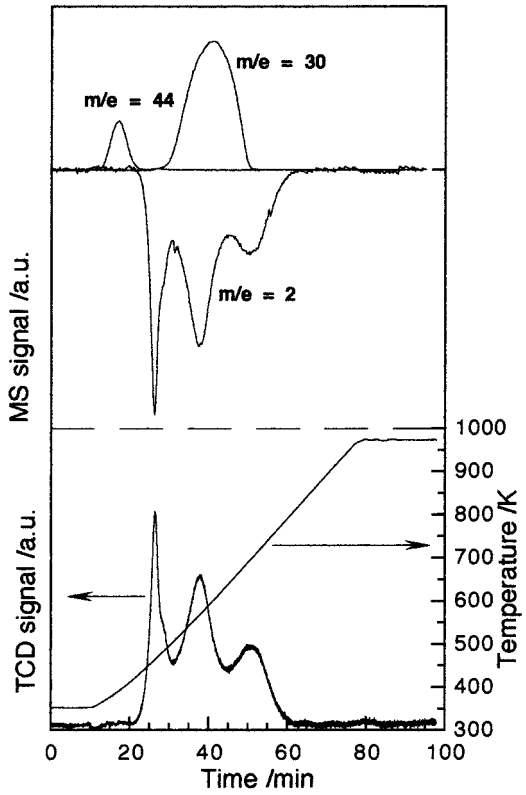

Figure 9. H_2-TPR profile followed by mass spectroscopy and TCD detection of Fe(97)BEA catalyst after oxidation in N_2O of the prereduced sample. Conditions, H_2/Ar (3/97); ramp, 10 K min^{-1}.

show any more H_2 consumption up to 900 K. Compared to samples calcined in air, the H_2 taken up by samples activated in N_2O is much more larger at low temperature. This is particularly true at low Fe content, with the appearance of several peaks of H_2 consumption below 573 K, which did not exist for the samples calcined in air. There is also a reduction peak at ca. 600−700 K in N_2O-treated samples, which merely corresponds to the reduction of binuclear oxocations in the O_2-treated samples, even if its shape and intensity appear somehow different. One may thus postulate some similarities between these latter oxocation species formed by either calcination or N_2O treatment.

Before definitely assigning these peaks to an actual H_2 consumption, it is advisable to check if any artifacts might occur from the desorption of nitrogen oxides species, such as N_2O and NO. It was recently shown by Xie and Lunsford[54] on Ba/MgO materials and by Holles et al.[55] on alumina-supported Pd and Rh that N_2O may disproportionate into N_2 and NO. To clarify that point, a H_2-TPR of Fe(97)BEAe was followed by TCD with an on-line MS coupling (Figure 9). It comes out that desorptions of N_2O ($m/e = 44$) and NO ($m/e = 30$) indeed occur at ca. 470 and 570 K, respectively. Nevertheless, the H_2-consumption profiles from TCD and MS ($m/e = 2$) superimpose very nicely, providing evidence that N_2O and NO desorptions do not affect the TCD signal in the H_2-TPR experiments. The H_2-TPR profiles in Figure 8 and H_2/Fe values reported in Table 4 then indeed correspond to the H_2 taken up by the samples.

The CO-TPR of N_2O-treated Fe−BEA confirms the occurrence of specific oxocations, reducible at lower temperature, formed by a specific interaction between Fe−BEA and N_2O. After calcination in air, the tendency was a decrease of H_2/Fe and CO/Fe values with the Fe content for Fe(*x*)BEAe (Table 1). In contrast, the reverse is true for the N_2O-treated samples, and both the H_2/Fe and CO/Fe values range between 0.5 and 1.0 as the Fe exchange level decreases.

From these experiments, it comes out that the fingerprint of the oxocations formed after N_2O-treatment is a facile reducibility even at low Fe content, the appearance of Lewis sites is likely in the vicinity of these oxocations, and high values of H_2/Fe (0.7−1.0) occur in the H_2-TPR of samples of low degrees of exhange. This specific surface O* formed by the interaction of N_2O with Fe^{2+} in BEA is very reactive and recalls immediately the "α-O" formed by the interaction of N_2O with Fe−ZSM-5.[1,16] The formation of "α-O" was claimed as the unique behavior of Fe−ZSM-5 and ferrosilicate analogues.[15] It is worth noting that the removal of this surface O* from Fe(*x*)BEAe is greatly helped by the addition of NH_3;[9,56] the light-off temperature of N_2O removal was indeed decreased by ca. 80 K. One can conceive that the adsorption of NH_3 on Lewis sites in close vicinity with the reactive surface O* makes easier its removal.

Several models have been designed for the architecture of this highly reactive oxocation formed by the interaction of N_2O with Fe−ZSM-5. Panov et al.[57] prompted by a biological model, the methane monooxygenase enzymes,[58] designed a binuclear Fe complex with various peroxide bridges. From ab initio quantum chemical calculations, Arbuznikov and Zhidomirov[59] confirmed the probability of similar binuclear oxocations with peroxide bridges and hydroxyl groups. Lazar et al.[14,18] also proposed an oxygen-bridge between two Fe atoms, one of the two belonging to the zeolite framework. The main problem associated with these models of a binuclear Fe complex is their probability of occurrence, which should decrease as the Fe content decreases too. This is not in line with the H_2-TPR and CO-TPR of N_2O-treated Fe(*x*)BEAe samples, since both H_2/Fe and CO/Fe values increase as Fe content decreases. From DFT computations, Yoshizawa et al.[60] proposed that "α-O" should have relevance to mononuclear iron−oxo species of the type $(FeO)^+$ on a AlO_4 surface site of ZSM-5 zeolite. It is clear that the debate about the exact nature of these sites remains still open in Fe−ZSM-5 catalysts. Moreover, compared to the rigidity of the ZSM-5 framework, the BEA is very flexible, which allows (i) reversible changes from tetrahedral to octahedral coordination of Al[20] and (ii) the presence of defects, dangling bonds, and partially coordinated aluminic fragments. Nevertheless, we can try to bring out some features about these Fe species:

(1) On the exchanged Fe−BEA calcined in air, we have concluded that the main species present are binuclear oxocations with FeOFe bridge (O/Fe = 0.5). These species could also be present in N_2O-treated Fe−BEA, though in lower proportions, and the H_2 consumption peak at ca. 600−700 K in H_2-TPR could be accounted for their reduction.

(2) The reduction peak at ca. 600−700 K in H_2-TPR of N_2O-treated Fe−BEA clearly tends to disappear at the benefit of the BT reduction peaks when the Fe content decreases. This is in agreement with a lower probability, from a statistical point of view, to form binuclear oxocations at low Fe content (vide

supra). Since the total H_2/Fe ratio then becomes larger than 0.5, we can reasonably propose that concurrently with the decrease of binuclear oxocations, there is the formation in higher proportion of mononuclear oxocations upon the treatment of Fe^{2+}−BEA with N_2O. These Fe complexes exhibit the higher reactivity with respect to H_2 and CO.

The exact nature of these species is still obscured. Studies by ESR spectroscopy and by quantum chemical calculations are in progress to elucidate that point.

IV. Conclusions

From classical ion-exchange procedures with $Fe(NO_3)_3$ and H−BEA, Fe can be introduced as Fe^{3+} up to a theoretical degree of exchange close to 100%. As soon as this theoretical degree of exchange exceeded 100%, amorphous Fe_2O_3 aggregates of small size are formed upon calcination in air. The Fe^{3+} charge compensation cations then transform into binuclear oxocations with FeOFe bridge (O/Fe = 0.5). The proportion of these species decreases with decreasing Fe content for statistical reasons. Fe species become hardly reducible, part of which can substitute Al in tetrahedral coordination.

The treatment by N_2O of Fe^{2+}−BEA, obtained from the reduction of exchanged and calcined samples, led to the formation of both mononuclear and binuclear Fe oxocations. The former are more easily reduced by H_2 and CO, and their formations are preferred at low Fe content.

Acknowledgment. M. M. is grateful to the "Ministère Français de l'Education Nationale, de la Recherche et de la Technologie" for a scholarship. The authors warmly thank A. Goursot and F. Fajula for helpful discussions.

References and Notes

(1) Panov, G. I.; Uriarte, A. K.; Rodkin, M. A.; Sobolev, V. I. *Catal. Today* **1998**, *41*, 365.
(2) Kapteijn, F.; Rodriguez-Mirasol, J.; Moulijn, J. A. *Appl. Catal., B* **1996**, *9*, 25.
(3) Feng, X.; Hall, W. K. *J. Catal.* **1997**, *166*, 368.
(4) Chen, H.-Y.; Sachtler, W. M. H. *Catal. Lett.* **1998**, *50*, 125.
(5) Yamada, K.; Pophal, C.; Segawa, K. *Microporous Mesoporous Mater.* **1998**, *21*, 549.
(6) Lobree, L. J.; Hwang, I.-C.; Reimer, J. A.; Bell, A. T. *Catal. Lett.* **1999**, *63*, 233.
(7) Kögel, M.; Sandoval, V. H.; Schwieger, W.; Tissler, A.; Turek, T. *Catal. Lett.* **1998**, *51*, 23.
(8) Long, R. Q.; Yang, R. T. *J. Am. Chem. Soc.* **1999**, *121*, 5595.
(9) Mauvezin, M.; Delahay, G.; Kieβlich, F.; Coq, B.; Kieger, S. *Catal. Lett.* **1999**, *62*, 41.
(10) Volodin, A. M.; Sobolev, V. I.; Zhidomirov, G. M. *Kinet. Catal.* **1998**, *39*, 775.
(11) Panov, G. I.; Sobolev, V. I.; Dubkov, K. A.; Kharitonov, A. S. *Stud. Surf. Sci. Catal.* **1996**, *101*, 493.
(12) Sobolev, V. I.; Panov, G. I.; Kharitonov, A. S.; Romannikov, V. N.; Volodin, A. M. *Kinet. Catal.* **1993**, *34*, 797.
(13) Ovanesyan, N. S.; Shteinman, A. A.; Dubkov, K. A.; Sobolev, V. I.; Panov, G. I. *Kinet. Catal.* **1998**, *39*, 792.
(14) Lazar, K.; Kotasthane, A. N.; Fejes, P. *Catal. Lett.* **1999**, *57*, 171.
(15) Kharitonov, A. S.; Sheveleva, G. A.; Panov, G. I.; Sobolev, V. I.; Paukshtis, Y. A.; Romannikov, V. N. *Appl. Catal., A* **1993**, *98*, 33.
(16) Dubkov, K. A.; Sobolev, V. I.; Panov, G. I. *Kinet. Catal.* **1998**, *39*, 72.
(17) Arbuznikov, A. V.; Zhidomirov, G. M. *Catal. Lett.* **1996**, *40*, 17.
(18) Lazar, K.; Lejeune, G.; Ahedi, R. K.; Shevade, S. S.; Kotasthane, A. N. *J. Phys. Chem. B* **1998**, *102*, 4865.
(19) Higgins, J. B.; Lapierre, R. B.; Schlenker, J. L.; Rohrman, A. C.; Wood, J. D.; Kerr, G. T.; Rohrbaugh, W. J. *Zeolites* **1988**, *8*, 446.
(20) Bourgeat-Lami, E.; Massiani, P.; Di Renzo, F.; Espiau, P.; Fajula, F.; Des Courrières, T. *Appl. Catal.* **1991**, *72*, 139.
(21) Pápai, I.; Goursot, A.; Fajula, F.; Weber, J. *J. Phys. Chem.* **1994**, *98*, 4654.
(22) Chen, H. Y.; Sachtler, W. M. H. *Catal. Today* **1998**, *42*, 73.
(23) Künding, W. *Nucl. Instrum. Methods Phys. Res., Sect. B* **1969**, *75*, 336.
(24) Krämmer, A.; Elidriss; Moubtassim, M. L.; Bousquet, C.; Olivier-Fourcade, J.; Jumas, J. C.; Tirado, J. L. *Nuevo Cimento* **1996**, *18*, 237.
(25) Unmuth, E. E.; Schwartz, L. H.; Butt, J. B. *J. Catal.* **1980**, *63*, 404.
(26) Brown, R.; Cooper, M. E.; Whan, D. A. *Appl. Catal.* **1982**, *3*, 177.
(27) Halawy, S. A.; Al-Shihry, S. S.; Mohamed, M. A. *Catal. Lett.* **1997**, *48*, 247.
(28) Lycourghiotis, A.; Vattis, D. *React. Kinet. Catal. Lett.* **1981**, *18*, 377.
(29) Wimmers, O. J.; Arnoldy, P.; Moulijn, J. A. *J. Phys. Chem.* **1986**, *90*, 1331.
(30) Pinna, F.; Fantinel, T.; Strukul, G.; Benedetti, A.; Pernicone, N. *Appl. Catal., A* **1997**, *149*, 341.
(31) Chen, K.; Fan, Y.; Hu, Z.; Yan, Q. *Catal. Lett.* **1996**, *36*, 139.
(32) Segawa, K.-I.; Chen, Y.; Kubsh, J. E.; Delgass, W. N.; Dumesic, J. A.; Hall, W. K. *J. Catal.* **1982**, *76*, 112.
(33) Schmidt, R.; Amiridis, M. D.; Dumesic, J. A.; Zelewski, L. M.; Millman, W. S. *J. Phys. Chem.* **1992**, *96*, 8142.
(34) Raj, A.; Sivasanker, S.; Lazar, K. *J. Catal.* **1994**, *147*, 207.
(35) Delgass, W. N.; Garten, R. L.; Boudart, M. *J. Phys. Chem.* **1969**, *73*, 2970.
(36) Lopez, A.; Lazaro, F. J.; Garcia-Palacios, J. L.; Larrea, A.; Pankhurst, Q. A.; Martinez, C.; Corma, A. *J. Mater. Res.* **1997**, *12*, 1519.
(37) Kündig, W.; Bömmel, H.; Conabaris, G.; Lindquist, R. H. *Phys. Rev.* **1966**, *142*, 327.
(38) Ratnasamy, P.; Kumar, R. *Catal. Today* **1991**, *9*, 328.
(39) Fyfe, C. A.; Strobl, H.; Kokotailo, G. T.; Pasztor, C. T.; Barlow, G. E.; Bradley, S. *Zeolites* **1988**, *132*, 8.
(40) Vaudry, F.; Di Renzo, F.; Fajula, F.; Schulz, Ph. *J. Chem. Soc., Faraday Trans.* **1998**, *94*, 617.
(41) Lei, G. D.; Adelman, B. J.; Sárkány, J.; Sachtler, W. M. H. *Zeolites* **1994**, *14*, 7.
(42) El-Malki, E.-M. E.; Santen, R. A. V.; Sachtler, W. M. H. *J. Phys. Chem. B* **1999**, *103*, 4611.
(43) Sobalik, Z.; Belhekar, A. A.; Tvaruzkova, Z.; Wichterlova, B. *Appl. Catal., A* **1999**, *188*, 175.
(44) Voskoboinikov, T. V.; Chen, H.-Y.; Sachtler, W. M. H. *Appl. Catal., B* **1998**, *19*, 279.
(45) Joyner, R. W.; Stockenhuber, M. *Catal. Lett.* **1997**, *45*, 15.
(46) Lobree, L. J.; Hwang, I.-C.; Reimer, J. A.; Bell, A. T. *J. Catal.* **1999**, *186*, 242.
(47) Novakova, J.; Kubelkova, L.; Witcherlova, B.; Juska, T.; Dolejsek, Z. *Zeolites* **1982**, *2*, 17.
(48) Flynn, C. M. *Chem. Rev.* **1984**, *84*, 31.
(49) Petunchi, J. O.; Hall, W. K. *J. Catal.* **1982**, *78*, 327.
(50) Garten, R. L.; Delgass, W. N.; Boudart, M. *J. Catal.* **1970**, *18*, 90.
(51) Fu, C. M.; Korchak, V. N.; Hall, W. K. *J. Catal.* **1981**, *68*, 166.
(52) Goursot, A.; Martines, A. Unpublished data.
(53) Mériaudau, P.; Naccache, C. *Appl. Catal.* **1991**, *73*, L13
(54) Xie, S.; Lunsford, J. H. *Appl. Catal., B* **1999**, *188*, 137.
(55) Holles, J. H.; Switzer, M. A.; Davis, R. J. *J. Catal.* **2000**, *190*, 247.
(56) Coq, B.; Mauvezin, M.; Delahay, G.; Kieger, S. *J. Catal.* **2000**, *195*, 298.
(57) Panov, G. I.; Sobolev, V. I.; Dubkov, K. A.; Parmon, V. N.; Ovanesyan, N. S.; Shilov, A. E.; Shteiman, A. A. *React. Kinet. Catal. Lett.* **1997**, *61*, 251.
(58) DeWitt, J. G.; Bentsen, J. G.; Rosenzweig, A. C.; Hedman, B.; Green, J.; Pilkington, S.; Papaefthymiou, G. C.; Dalton, H.; Hodgson, K. O.; Lippard, S. J. *J. Am. Chem. Soc.* **1991**, *113*, 9219.
(59) Arbuznikov, A. V.; Zhidomirov, G. M. *Catal. Lett.* **1996**, *40*, 17.
(60) Yoshizawa, K.; Shiota, Y.; Yumura, T.; Yamabe, T. *J. Phys. Chem. B* **2000**, *104*, 734.